VJQBB | Vol 1, Issue 1 | 2026 | Article 001

Perspective Article

Virosa Journal of Quantum Biology and Biomedicine

Quantum Health: A Painlevé Geometric Framework for Biological Regulation, Disease, and Recovery

Michel Planat [a]

[a] *Institut FEMTO-ST CNRS UMR 6174 , Université Marie et Louis Pasteur, Besançon, France.*

Keywords:

Quantum health, Nonlinear dynamics in biology, Painlevé equations, Bifurcation and disease, Epithelial-mesenchymal transition, MicroRNA regulatory networks, Cancer dormancy.

ABSTRACT

We propose a mathematically grounded framework for biological regulation, health, and disease based on the confluence hierarchy of Painlevé equations and the decorated character varieties introduced by Chekhov, Mazzocco, and Rubtsov. The sixth Painlevé equation (PVI), associated with the four-punctured sphere and cusp signature (0, 0, 0, 0), describes a progenitor regulatory manifold in which four independent dynamical flows interact without binding. The confluence PVI→PV in which two singularities merge and two cusps appear on a shared boundary component, yielding cusp signature (0, 0, 2) models the emergence of a bipolar regulatory state a two-level system analogous to a quantum bit, capable of switching between competing physiological regimes.

From this critical state, three inequivalent degeneration channels arise. The balanced channel PIII(D_6), with signature (0, 2, 2), represents a stable homeostatic attractor that we identify with quantum health, robust, self-correcting biological regulation. The degenerate channel PV_{deg}, with signature (0, 0, 1), corresponds to a metastable chronic-disease state that shares the same underlying character variety as PIII(D_6) yet is dynamically confined a phenomenon we term the autistic trap, paralleling the regulatory lock-in observed in cancer dormancy, chronic inflammation, and neurodegenerative persistence. The hyper-binding channel PIV, with signature (0, 4), models catastrophic regulatory collapse such as aggressive oncogenesis or acute systemic failure. A recovery pathway from PV_{deg} to PIII(D_7) which preserves all three flows with cusp signature (0, 1, 2) represents what we call Nash recovery: a term introduced not in reference to Nash's game theory but to his documented personal recovery from paranoid schizophrenia, the archetypal escape from a metastable cognitive trap into a reorganized, stable equilibrium. The integrative D-type pathway $D_6 \rightarrow D_7$ further deepens healthy regulation toward the creative flow state D_8 (signature (0, 1, 1)).

This framework is anchored to specific biological evidence: microRNA-mediated gene regulatory networks exhibit moduli-space geometry consistent with character varieties; Painlevé V appears in the density matrix of correlated quantum systems and in level-spacing statistics relevant to noise in living cells and PV dynamics has been linked to gamma-oscillation consciousness models that bear on health. We argue that cusp signatures provide a new class of topological biomarkers for distinguishing dynamical regimes of biological regulation, with implications for diagnostics, therapeutic targeting, and the mathematical unification of health science.

1. Introduction

Health is a dynamical phenomenon. Modern systems biology has established that living organisms maintain stability not through rigid molecular blueprints but through attractors of nonlinear dynamical systems self-correcting trajectories embedded in high-dimensional state spaces [1-3]. Disease, accordingly, is not a simple deficiency but a transition to an alternative dynamical regime, often reached through a cascade

* Corresponding author: Michel Planat, Institut FEMTO-ST CNRS UMR 6174 , Université Marie et Louis Pasteur, Besançon, France, *E-mail address*: michel.planat@femto-st.fr

Received: 19 March 2026; **Accepted:** 26 March 2026; **Published:** on 16 April 2026

Citation: Planat M. Quantum Health: A Painlevé Geometric Framework for Biological Regulation, Disease, and Recovery. Virosa J Quantum Biol Biomed (VJQBB). 2026;1(1):1-11.

of bifurcations rather than by a single catastrophic failure [4,5]. This perspective opens the possibility of describing health and disease in geometric terms as positions and movements within a structured mathematical landscape.

At the same time, two complementary fields offer striking mathematical tools. Quantum biology has demonstrated that quantum-mechanical processes coherent energy transfer in photosynthesis, radical-pair magneto reception, proton tunneling in enzyme catalysis play functional roles in living systems [6,7]. Whether or not these specific quantum mechanisms extend to regulatory networks, they motivate the search for deep mathematical structures shared between physics and biology. In parallel, the theory of Painlevé equations provides exactly such structures, a hierarchy of nonlinear differential equations that govern critical phenomena across statistical mechanics, random matrix theory, quantum field theory, and integrable systems [8] and whose topological classification via character varieties and cusp signatures has recently been placed on a rigorous footing by Chekhov, Mazzocco, and Rubtsov [9].

The present work brings these threads together. In [10], algebraic geometry methods revealed that microRNA (miRNA) regulatory networks in health and disease are classified by moduli spaces closely related to character varieties. In [11], the authors showed that the qubit arises naturally from the Painlevé V confluence as a topological critical state, whose three degeneration channels carry geometrically distinct cusp signatures. In [12,13], Painlevé V dynamics was linked to gamma oscillation models of consciousness, with bifurcation channels corresponding to distinct cognitive and psychiatric states.

Building on these foundations, we propose a unified Quantum Health framework a geometric map of biological regulation in which health, chronic disease, acute disease, and recovery correspond to specific nodes and trajectories in the Painlevé confluence diagram, discriminated by their cusp signatures. The framework is conceptual but anchored to measurable quantities: cusp signatures are topological invariants that may in principle be extracted from network topology, correlation functions, and time-series data of biological systems near critical transitions.

The paper is organized as follows. Section 2 reviews the Painlevé hierarchy, character varieties, and the cusp-signature classification of Chekhov, Mazzocco and Rubtsov. Section 3 explains how the PVI→PV confluence produces a biological analogue of the qubit. Section 4 develops the Quantum Health phase diagram, with each node of the Painlevé tree mapped to a specific physiological regime and supported by biological evidence. Section 5 connects the framework to miRNA regulatory networks and character variety geometry. Section 6 analyses the autistic trap and its biological manifestations. Section 7 develops the theory of Nash recovery. Section 8 discusses the link between Painlevé dynamics, consciousness, and health. Section 9 outlines experimental and theoretical directions. Section 10 concludes.

2. The Painlevé Hierarchy, Character Varieties, and Cusp Signatures

2.1. Painlevé equations and the confluence diagram

The six classical Painlevé equations (PI through PVI) form a hierarchy connected by confluence processes, in which singularities of the governing differential equation are merged by a controlled limit procedure. The most general member, PVI, is associated with a linear Fuchsian system on the four-punctured sphere $P^1\backslash\{0, 1, t,\infty\}$ and governs isomonodromic deformations of flat SL(2,C) connections [17,18]. All other Painlevé equations arise from PVI through successive confluences [19,20].

$$\mathrm{PVI} \longrightarrow \mathrm{PV} \longrightarrow \begin{cases} \mathrm{PIII}(D_6) \longrightarrow D_7 \longrightarrow D_8 & \text{(D-type integrative path)} \\ \mathrm{PV}_{\mathrm{deg}} & \text{(E-type: autistic trap)} \\ \mathrm{PIV} & \text{(E-type: collapse)} \end{cases} \quad (1)$$

A key physical fact motivating this hierarchy: the fifth Painlevé transcendent appears explicitly in the exact computation of the density matrix of the one-dimensional impenetrable Bose gas [21] and in the gap probability of the Gaussian unitary ensemble [22,23]). These are not metaphors, they are analytical results in established physics, suggesting that PV governs universal critical behavior in correlated many body systems a class that plausibly includes the gene-regulatory and signaling networks of living cells.

2.2. Fricke character varieties

Each Painlevé equation is associated with a moduli space of flat SL(2,C) representations, known as the Fricke character variety [24]. For PVI, associated with the four-punctured sphere, this variety is described by the Fricke-Vogt relation.

$$X_1X_2X_3 + X^2_1 + X^2_2 + X^2_3 = K_1X_1 + K_2X_2 + K_3X_3 + K_4 \quad (2)$$

Where X_i are traces of monodromy matrices and K_i are parameter combinations [25]. Character varieties encode the global topology of the dynamical constraints governing a system. They are the configuration spaces within which trajectories evolve. A deeper interpretation of the parameters K_i in (2) is provided by the identification of Painlevé equations with four-dimensional integrable systems [16], the K_i correspond to independent coupling strengths between regulatory components the biological analogues of mass parameters. Changes in these coupling strengths due to miRNA dysregulation correspond to deformations of the regulatory phase space, placing transitions between health and disease within a precisely structured mathematical landscape in which the reachable dynamical states are topologically constrained.

2.3. Cusp signatures and decorated character varieties

The decorated character variety classification of Chekhov, Mazzocco and Rubtsov [9] assigns to each Painlevé equation a bordered Riemann surface characterized by the number of holes

(independent dynamical flows) and the distribution of cusps among boundary components.

Table 1: Painlevé equations and their cusp signatures in the Chekhov-Mazzocco-Rubtsov decorated character variety classification [9]. The number of holes records independent dynamical flows; cusps record binding sites between flows.

Equation	Holes	Cusps	Signature	Dynamical character
PVI	4	0	(0, 0, 0, 0)	Progenitor; 4 independent flows
PV	3	2	(0, 0, 2)	Bipolar critical state; qubit node
PIII(D_6)	3	4	(0, 2, 2)	Balanced; symmetric cusp distribution
PV_{deg}	3	1	(0, 0, 1)	Degenerate; same variety as D_6
PIV	2	4	(0, 4)	Hyperbinding; one flow collapsed
PIII(D_7)	3	3	(0, 1, 2)	Nash recovery; 3 flows, unbalanced rebalancing
PIII(D_8)	3	2	(0, 1, 1)	Creative flow; 3 flows, minimal balanced binding

Cusps record the degree of binding between flows, Zero cusps means four independent interactions (PVI), while accumulation of cusps signals progressive constraint or collapse of the interaction structure. The key result exploited here is: PIII(D_6) and PV_{deg} share the same underlying character variety but carry different cusp signatures, meaning they are geometrically indistinguishable at the algebraic level yet dynamically distinct. This fact has profound biological consequences, as we shall see.

3. The PVI→PV Confluence as Biological Qubit Transition

3.1. The prequbit state: PVI as regulatory progenitor

The PVI regime, with signature (0, 0, 0, 0), describes a system with four punctures on the Riemann sphere and no cusps: four independent monodromy flows without mutual binding. In a biological context, this represents an undifferentiated or progenitor regulatory state a pluripotent configuration in which multiple signaling pathways operate in parallel without committing to a particular dynamical regime. Examples include embryonic stem cells prior to differentiation commitment, tissue progenitor cells, or the multi-attractor landscape of an immune system at rest, maintaining simultaneous readiness across multiple effector pathways.

3.2. The PV critical state: emergence of bipolarity

The confluence PVI→PV merges two of the four singular points. In the Chekhov, Mazzocco and Rubtsov classification, this reduces the configuration from four holes and zero cusps to three holes and two cusps on a shared boundary component, yielding signature (0, 0, 2). The two cusps create competing binding sites along the interaction channel, generating an irreducible bipolar structure. This is the mathematical definition of a qubit [11], a system in which two competing configurations interact across a shared interface.

A crucial physical property accompanies the PV critical state: it is precisely at this node that the power spectrum of dynamical fluctuations exhibits a 1/f (flicker noise) signature, the universal spectral hallmark of systems operating at the edge of integrability [14]. This 1/f spectrum emerges from the WKB/Stokes analysis of Painlevé V confluence, the singularity separation $\Delta(t) \to 0$ generates an instantaneous frequency scaling as $\omega(\tau) \sim C\tau^{-1/2}$, whose Fourier power spectral density scales as $S(f) \propto 1/f$. In the Bost-Connes quantum statistical model, this corresponds to the critical inverse temperature $\beta \approx 1$, the pole of the Riemann zeta function $Z(\beta) = \zeta(\beta)$, where spontaneous symmetry breaking and maximal arithmetic fluctuations coincide. In biology, this means that systems near the PV critical transition (bistable decision points) should generically exhibit 1/f noise in the fluctuations of their regulatory outputs a measurable prediction. In biological terms, the PV state corresponds to systems committed to bistable regulatory decision points:

1. ***Cell fate commitment***: the p^{53}-MDM_2 negative feedback loop generates discrete digital pulses of p^{53} whose number encodes damage severity, ultimately driving the cell toward either arrest or apoptosis [27]. The bistable switch between these two outcomes has been characterised in computational models of the p^{53} network as a bifurcation between coexisting stable attractors [28,29].

2. ***Epithelial-mesenchymal transition (EMT) as a four-component PV qubit system***: Nieto et al. [30] identified the core regulatory machinery of EMT as two coupled double negative feedback axes: the miR-200/ZEB1-ZEB2 axis and the miR-34/SNAI1 axis. In the miR-200/ZEB axis, the five members of the miR-200 family (miR-200a/b/c, miR-141, miR-429) suppress translation of ZEB1 and ZEB2 mRNAs, while ZEB1/2 reciprocally repress miR-200 gene transcription [31]. In the miR-34/SNAI1 axis, miR-34 family members repress SNAI1 (Snail), while SNAI1 represses miR-34 transcription. These two axes are themselves coupled through ZEB1-SNAI1 cross-regulation and shared TGF-β input.

   This two-axis, four-component architecture is precisely the structure of the PV regulatory system. The three independent parameters of the PV equation correspond directly to the three independent coupling strengths of the EMT network [16], the strength θ_0 of the miR-200/ZEB axis, the strength θ_t of the miR-34/SNAI1 axis, and their inter-axis coupling θ_*. The cusp signature (0, 0, 2) of PV encodes the two competing stable attractors (epithelial and mesenchymal) sharing a common interaction boundary through which all four regulatory components communicate.

   Crucially, the PV critical state exhibits two structurally distinct dynamical regimes that coexist and alternate over time. In the committed regime, the cell resides in a stable epithelial or mesenchymal state, the four components are present but a single collective order parameter (E-cadherin level, or ZEB1 level) captures the dominant dynamics, with the individual axis strengths contributing only sub-leading corrections. In the

transitional regime, the cell occupies the hybrid E/M state: all four regulatory components are simultaneously active and equally weighted, with the inter-axis coupling θ_* amplifying any imbalance between the two axes. The alternation of a cell population between these two regimes, with dwell-time distribution $P(\tau) \sim \tau - 1$ characteristic of the PV confluence [14], generates the 1/f fluctuation spectrum that is the universal dynamical signature of the EMT decision node. The spectral exponent α in $S(f) \propto 1/f\alpha$ therefore serves as a topological biomarker: $\alpha \approx 1$ identifies hybrid E/M cells at maximal plasticity, while deviations from unity indicate distance from the PV critical point in either direction.

Nieto et al. [30] established that the hybrid E/M state carries the highest degree of plasticity and the highest cancer stem cell potential cells simultaneously possessing epithelial and mesenchymal traits. In the Painlevé picture, this maximal plasticity arises directly from the four-component transitional structure: it is the only regime where all regulatory inputs are simultaneously decisive, making these cells maximally sensitive and responsive to micro-environmental signals. The three degeneration channels from PV correspond directly to EMT outcomes, D_6 (healthy epithelial homeostasis, balanced dual-axis regulation), PV_{deg} (the autistic trap of partial or hybrid EMT stabilised by autocrine TGF-β and reversible CpG methylation of miR-200 loci, which preserves the two-axis topology but collapses the cusp balance, preventing spontaneous reversion); and PIV (complete irreversible mesenchymal commitment with constitutive silencing of miR-200 and aggressive metastatic invasion). Reversibility through mesenchymal to epithelial transition (MET) enabling colonisation at distant sites corresponds to Nash recovery ($PV_{deg} \rightarrow D_7$), a reorganized, partially re-epithelialised stable state with one surviving dominant regulatory axis, distinct from the original primary tumor phenotype.

Therapeutically, miR-200 mimics, TGF-β inhibitors, and DNMT inhibitors act as cusp signature modulators, they preserve the underlying character variety but shift the cusp distribution sufficiently to restore access to the epithelial or D_7 attractor. The prediction that combined miR-200 mimic and miR-34 mimic therapy should show synergy specifically in hybrid E/M cells (where both axes are active at leading order) but not in committed cells follows directly from the four-component structure of the transitional regime.

3. ***Immune checkpoint states***: T-cell exhaustion versus effector activation represents a bistable PV-type configuration [32], with therapeutic immune checkpoint blockade providing the perturbation that tips the system between states.

The PVI→PV transition therefore models the loss of pluripotency and commitment to a two alternative decision the critical moment at which a regulatory system acquires the capacity to switch between health and disease 72 hours, the following staining assays were carried out for analysis.

4. Quantum Health: The Painlevé Phase Diagram of Biological Regulation

4.1. MMT Dye assay using ELISA

From the bipolar PV state, three inequivalent degeneration channels emerge (*Figure. 1*). These are not merely abstract mathematical alternatives: each channel carries a distinct cusp signature that encodes a qualitatively different reorganisation of the interaction structure, invisible at the level of algebraic character varieties alone.

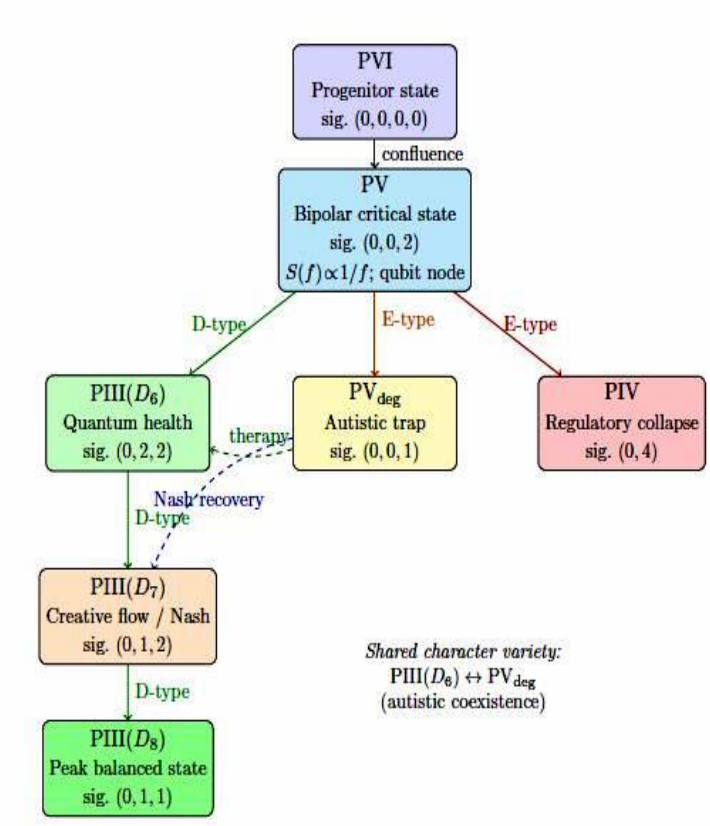

Figure 1: Full Quantum Health phase diagram following the complete Chekhov–Mazzocco–Rubtsov Painlevé tree [9,12]. PV is the bipolar critical node at which 1/f noise and qubit dynamics emerge. The D-type integrative pathway (green solid arrows) deepens health: $D_6 \rightarrow D_7 \rightarrow D_8$, preserving all three flows while progressively balancing cusp distribution. PV_{deg} (yellow): autistic trap sharing the same character variety as D_6. PIV (red): catastrophic regulatory collapse. Dashed blue: Nash recovery ($PV_{deg} \rightarrow D_7$), named after John Nash's life trajectory of recovery from schizophrenia. Dashed green: direct therapeutic restoration ($PV_{deg} \rightarrow D_6$).

4.2. Channel 1: PIII(D_6) Quantum health and the D-type integrative pathway

The balanced channel carries signature (0, 2, 2), three holes with

four cusps symmetrically distributed between two boundary components. This symmetric redistribution stabilizes the interaction structure while preserving three independent dynamical flows. We identify this regime with quantum health: a state in which regulatory networks are stable, self-correcting, and resistant to moderate perturbations.

Definition 1 (Quantum health). Quantum health is the dynamical regime corresponding to the PIII(D_6) Painlevé equation, characterised by cusp signature (0, 2, 2), in which a biological regulatory network maintains a balanced attractor with multiple interacting but symmetrically coupled degrees of freedom.

The D_6 configuration is the entry point of the full D-type integrative pathway identified in the complete Chekhov tree [9,12].

$$\mathbf{D_6\ (0,\ 2,\ 2) \rightarrow D_7\ (0,\ 1,\ 2) \rightarrow D_8\ (0,\ 1,\ 1)} \qquad \mathbf{(3)}$$

Each step along this path reduces the total cusp count while maintaining all three independent flows and progressively rebalancing the cusp distribution. D_7, with three holes and three cusps in signature (0, 1, 2), represents a creative-flow or expert health state: slightly less rigid than D_6 (one fewer cusp on one boundary) but equally stable and capable of sustained high-level function. D_8, with signature (0, 1, 1), achieves minimal perfect balance, the simplest possible symmetric cusp distribution preserving all flows, corresponding to seamless, effortless physiological integration at its most refined. In clinical terms, the $D_6 \rightarrow D_7 \rightarrow D_8$ continuum represents the gradation from robust normal homeostasis through peak physiological performance to exceptional regulatory integration, as might be observed in highly trained athletes, long-meditated nervous systems, or exquisitely calibrated immune responses.

Biological hallmarks of this state:

1. ***Homeostatic robustness***: the ability to return to a stable set point after perturbation, as exemplified by blood glucose regulation via the insulin-glucagon-incretin axis, where multiple feedback loops maintain normoglycaemia across wide ranges of dietary input [40].

2. ***miRNA buffering***: healthy miRNA networks function as noise-damping regulators; the redundant targeting of common mRNAs by multiple miRNA's (e.g., the coherent feed-forward motifs involving miR-21, miR-155, and miR-146a in innate immunity) maintains signaling fidelity [26].

3. ***Waddington landscape analogy***: In Waddington's epigenetic landscape, the D_6 regime corresponds to a cell resting in a deep, wide potential well a stable cell type attractor such as terminally differentiated hepatocytes, cardiomyocytes, or memory T cells, each characterized by robustly maintained chromatin states [3,39].

4.3. Channel 2: PV_{deg} -The autistic trap (metastable chronic disease)

The degenerate channel carries signature (0, 0, 1), three holes but only a single cusp, meaning the bipolar binding geometry has collapsed to a single constraint. The system retains the same underlying character variety as PIII(D_6) it is geometrically within reach of the healthy state yet is dynamically confined to a suboptimal configuration. Section 6 analyses this phenomenon in detail.

4.4. Channel 3: PIV- Regulatory collapse

The hyperbinding channel carries signature (0, 4), only two holes remain (one independent flow has been eliminated entirely) while all four cusps concentrate on a single boundary component. This extreme constraint of the interaction geometry corresponds to catastrophic loss of regulatory flexibility.

In biology, the PIV regime models:

1. ***Oncogenic transformation***: The constitutive activation of Ras-MAPK-ERK signaling (observed in approximately 30% of human cancers [36]) represents a PIV-type configuration, a single dominant drive overrides the normal multiplicity of regulatory inputs, locking the cell into uncontrolled proliferation.

2. ***Cytokine storm***: In severe COVID-19 or sepsis, the positive feedback amplification of IL-6 and TNF-α collapses immune regulatory architecture into a single hyper-binding attractor of runaway inflammation [37].

3. ***Acute neurological crises***: Status epilepticus, in which sustained seizure activity overwhelms inhibitory regulatory circuits, exhibits the signature of PIV collapse, multiple independent circuit flows replaced by a single dominant hypersynchronous mode [38].

4.5. The phase diagram: a summary

Table 2 maps the full Painlevé hierarchy to biological states, cusp signatures, and representative pathological or healthy examples.

Table 2: The Quantum Health phase diagram: Painlevé equations, cusp signatures, and biological states.

Equation	Signature	Biological state	Representative examples
PVI	(0, 0, 0, 0)	Pluripotent/undifferent	Embryonic stem cells, naive immune precursors
PV	(0, 0, 2)	Critical transition	EMT switch, p53 checkpoint, T-cell exhaustion threshold

PIII(D_6)	(0, 2, 2)	Quantum health, homeostasis	Normoglycaemia, immune Memory, terminal differentiation
PV_{deg}	(0, 0, 1)	Autistic trap, chronic disease	Metabolic syndrome, cancer Dormancy, chronic neuroinflammation
PIV	(0, 4)	Regulatory collapse, acute disease	Oncogenic transformation, cytokine storm, status epilepticus
PIII(D_7)	(0, 1, 2)	Nash recovery, creative flow	Post-treatment remission, Neuroplasticity, postschizophrenic recovery
PIII(D_8)	(0, 1, 1)	Peak balanced Health, deep integration	Optimal homeostasis, expert regulatory coherence

5. microRNA Networks, Character Varieties, and Quantum Health

5.1. miRNA regulatory networks as geometric objects

MicroRNA's are small (∼22 nt) non-coding RNA molecules that repress gene expression post transcriptionally by binding to complementary sequences in the 3′ UTR of target mRNAs [26]. A single miRNA typically targets hundreds of mRNAs; conversely, a single mRNA may be regulated by dozens of miRNA's. The resulting regulatory architecture is a dense, multiply connected network with emergent dynamical properties not predictable from individual interactions.

In [10], it was shown that the moduli spaces associated with miRNA regulatory networks in health and disease carry algebraic geometric structure closely related to SL(2,C) character varieties. Specifically, the braid group representations underlying miRNA network topology generate constraints equivalent to Fricke-type relations (2), placing these biological networks within the same mathematical framework as Painlevé equations.

This is not merely a formal analogy. The parameters K_i appearing in the character variety correspond to specific miRNA-mRNA interaction strengths and network connectivity measures. Changes in these parameters corresponding to altered miRNA expression in disease correspond to movements in the moduli space, and therefore to transitions between Painlevé regimes.

5.2. Specific miRNA-disease transitions and cusp signatures

Several well characterised miRNA dysregulation events in cancer and metabolic disease can be tentatively mapped to Painlevé transitions:

1. ***miR-21 upregulation in cancer ($D_6 \rightarrow PV_{deg}$ or PIV):*** miR-21 is the most consistently overexpressed miRNA across human cancers [33]. It suppresses PTEN and $PDCD_4$, releasing PI3K-Akt signalling from inhibitory constraint. In the Painlevé picture, this corresponds to a cusp collapse: the symmetric inhibitory architecture (D_6) is disrupted, and the network transitions toward either the autistic trap (PV_{deg}, early tumorigenesis with maintained dormancy) or catastrophic PIV collapse (invasive disease with MAPK co-activation).

2. ***The miR-200/ZEB axis in EMT (PVI→ PV):*** The bistable switch governing epithelial mesenchymal transition is controlled by mutual inhibition between the miR-200 family (miR-200a/b/c, miR-141, miR-429) and the ZEB1/ZEB2 transcription factors [30]. This double negative feedback creates a canonical PV-type qubit from an initial more complex regulatory manifold a PVI→PV transition that determines metastatic potential.

3. ***miR-155 in inflammatory disease ($D_6 \rightarrow PV_{deg}$):*** In chronic inflammatory conditions (rheumatoid arthritis, inflammatory bowel disease), sustained miR-155 up-regulation maintains NF-κB signalling in a persistently activated state despite the presence of intact regulatory mechanisms [34]. This is a prototypical autistic trap: the character variety is preserved (the regulatory architecture is intact) but the cusp signature has collapsed from the symmetric (0, 2, 2) of healthy immune regulation to the degenerate (0, 0, 1) of chronic inflammatory drive. miR-7 and insulin signaling in type 2 diabetes ($D_6 \rightarrow PV_{deg}$): miR-7-2 regulation of the insulin receptor and IRS-2 pathway in pancreatic β-cells demonstrates how modest dysregulation of a single miRNA node can induce a metastable state (impaired but not absent insulin secretion) consistent with the autistic trap phenomenology [35].

These examples illustrate that the Painlevé framework provides a language for classifying miRNA-driven disease transitions by their topological character (which cusp signature is induced) rather than solely by their molecular identity.

5.3. Character varieties as regulatory phase spaces

The identification of biological regulatory networks with character varieties implies that the global topology of the regulatory landscape its fundamental group structure, its singularities, its monodromy constrains the set of reachable dynamical states. This is a stronger statement than typical systems biology: it asserts not merely that certain dynamics are difficult to achieve, but that they are topologically inaccessible from a given

initial configuration without passing through a well-defined critical point.

This topological constraint may explain several puzzling features of biological regulation:

1. The robustness of healthy cell type identities against moderate perturbations (the topology of D_6 protects the attractor).

2. The remarkable difficulty of reprogramming differentiated cells to pluripotency without specific transcription factor cocktails [41] (Yamanaka reprogramming corresponds to a topological transition from D_6 back toward PVI, requiring specific cusp-generating perturbations).

3. The phenomenon of oncogene addiction, in which cancer cells paradoxically require the continued activity of the very oncogene that initiated their transformation (the PIV topology, once established, cannot be escaped without either reverting the collapsed flow or accessing an entirely different confluence pathway).

6. The Autistic Trap: Dynamical Confinement in a Shared Character Variety

6.1. Coexistence without identity

The most striking consequence of the cusp signature classification is the relationship between PIII(D_6) and PV_{deg}, they share the same underlying character variety while carrying different cusp signatures [9,11]. Algebraically, the two states are indistinguishable. Dynamically, they are fundamentally different.

We call this the autistic trap, a situation in which the system occupies a dynamical configuration that is geometrically embedded within the healthy attractor's configuration space yet is confined by its cusp structure to a suboptimal regime. The term reflects the concept of a system that "can see" the healthy state in the algebraic sense but cannot access it dynamically not through lack of capability, but through topological confinement.

A structural explanation for the resistance of the autistic trap to incremental perturbations emerges from the mathematical properties of the D_6/PV_{deg} degeneracy. The two configurations, though sharing the same character variety, are separated by a singular reorganization of the cusp structure: escaping from PV_{deg} to D_6 requires the system to pass through this singular point [16], analogous to crossing a phase boundary rather than sliding continuously along an attractor. Weak perturbations modest changes in a single miRNA level, minor metabolic corrections, and incremental pharmacological doses provide insufficient structural energy to cross this barrier, explaining the well documented clinical observation that chronic inflammatory states, dormant cancers, and metabolic syndrome resist gradual intervention. By contrast, sufficiently large perturbations that simultaneously reorganize multiple regulatory interactions (bariatric surgery, high-intensity combination epigenetic therapy, complete immune checkpoint blockade) can succeed precisely because they provide enough energy to traverse the singular reorganization point and reach the D_6 basin.

Remark 1. *The terminology "autistic" here is mathematical and metaphorical, describing a specific topological phenomenon. It is not intended to characterize the neurological condition of autism spectrum disorder, which has its own distinct biological basis. The mathematical autistic trap applies to any biological system exhibiting the D_6/PV_{deg} coexistence structure.*

6.2. Biological manifestations of the autistic trap

6.2.1. Cancer dormancy and minimal residual disease

One of the most clinically significant manifestations of the autistic trap is cancer dormancy: the persistence of residual tumour cells in a quiescent, non-proliferating state following apparently successful treatment [42]. Dormant cancer cells maintain a regulatory architecture superficially indistinguishable from healthy cells (they express tissue-appropriate surface markers, do not proliferate, are not recognised as foreign) yet remain primed to re-awaken into active disease.

In the Painlevé picture:

1. The healthy normal cell resides in PIII(D_6) with signature (0, 2, 2).

2. The dormant cancer cell occupies PV_{deg} with signature (0, 0, 1) the same character variety, a different cusp structure that maintains the cell in a metastable state without pushing it to PIV collapse.

3. Re-awakening corresponds to the $PV_{deg} \rightarrow$ PIV transition, often triggered by micro environmental cues (immune suppression, angiogenic factors, and physical disruption of stromal architecture).

The autistic trap model predicts that distinguishing dormant tumour cells from healthy stromal cells may require topological biomarkers measures sensitive to cusp signatures rather than standard molecular markers and that de-stabilising the metastable state toward PIV (e.g., through wound-healing inflammation or immune senescence) is what triggers relapse.

6.2.2. Chronic low-grade inflammation

Chronic low-grade inflammation in metabolic syndrome, type 2 diabetes, and non-alcoholic fatty liver disease exhibits the autistic trap phenomenology [43]:

1. Inflammatory biomarkers (IL-6, TNF-α, CRP) are elevated but not at the acute levels seen in PIV collapse.

2. The regulatory infrastructure remains architecturally intact (adaptive immune responses are mounted, resolution pathways exist).

3. Yet the system is stably confined in a PV_{deg} state from which ordinary regulatory activity cannot escape.

Interventions that successfully resolve metabolic inflammation (caloric restriction, exercise, bariatric surgery, GLP-1 agonists) may be interpreted as cusp-signature-modifying perturbations, they alter the topological structure of the regulatory landscape sufficiently to permit re-entry into the D_6 basin of attraction.

6.2.3. Epigenetic memory and transcriptional locking

In development and cancer, the concept of epigenetic locking the persistence of aberrant gene expression patterns despite the availability of corrective signaling [44] corresponds precisely to the autistic trap. CpG island hypermethylation of tumour suppressor genes (e.g., p16INK4a, RASSF1A, BRCA1) in cancer cells does not eliminate the regulatory machinery governing these genes; it confines the epigenetic state to a PV_{deg} configuration in which the corrective pathway is topologically inaccessible without epigenetic reprogramming.

DNA methyltransferase inhibitors (e.g., 5-azacytidine) and HDAC inhibitors can be understood as cusp-signature modulators: they do not change the character variety (the underlying gene network topology is preserved) but alter the cusp distribution sufficiently to permit access to the D_6 attractor.

7. Nash Recovery: The $PV_{deg} \rightarrow PIII(D_7)$ Transition

7.1. The $PIII(D_7)$ configuration

The autistic trap model predicts that distinguishing dormant tumour cells from healthy stromal cells may require topological biomarkers measures sensitive to cusp signatures rather than standard molecular markers and that destabilising the metastable state toward PIV (e.g., through wound-healing inflammation or immune senescence) is what triggers relapse.

Mathematically, D_7 corresponds to a system with precisely one surviving free parameter one dominant regulatory axis around which the other interactions have re-organised [16]. The asymmetric signature (0, 1, 2) is a direct consequence: one boundary component carries two binding sites (the dominant axis), the other carries one (the re-organised secondary interaction). This single parameter structure provides a topological explanation for why Nash recovery produces a state that is irreversibly distinct from the original D_6 health, the asymmetry introduced by the single surviving dominant parameter cannot be erased without a further topological transition. In clinical terms, the dominant surviving axis may be structural connectivity in post-stroke neuroplasticity, residual immune memory in cancer remission, or stromal architecture in wound healing each leaving an indelible asymmetric imprint on the recovered state.

We term the transition $PV_{deg} \rightarrow PIII(D_7)$ Nash recovery, The name refers not to Nash's game-theoretic equilibrium concept but to John Nash's personal life trajectory: his documented recovery from paranoid schizophrenia exemplifies the escape from a metastable degenerate state (PV_{deg}, the autistic trap of psychosis) to a re-organised, functioning equilibrium (D_7) achieved not by returning to the pre-illness state but by finding a new mode of cognitive engagement [12]. The Nash path also connects to the D-type integrative route: a system recovering through D_7 can continue toward D_8, the peak balanced state.

Definition 2 *(Nash recovery). Nash recovery is the dynamical transition from PV_{deg} (the autistic trap, signature (0, 0, 1)) to $PIII(D_7)$ (signature (0, 1, 2), three flows preserved): the escape from metastable confinement to a re-organised but stable configuration with enriched and partially rebalanced cusp structure. The term honours John Nash's personal recovery trajectory rather than any game-theoretic construction.*

7.2. Biological instances of Nash recovery

7.2.1. Wound healing and tissue regeneration

Tissue repair following injury follows a stereotyped sequence: haemostasis, inflammation, proliferation, re-modelling. This sequence is not a return to the pre-injury state (D_6) but a transition through a series of intermediate states (some of which are PV_{deg} type metastable configurations: the proliferating fibroblast state, the myofibroblast transition toward a stable re-modelled state that may include scar tissue [45]. This final state functionally stable but architecturally distinct from the original tissue is the biological analogue of $PIII(D_7)$.

7.2.2. Cancer remission and immune remodelling

Complete pathological response to cancer therapy (chemotherapy, immunotherapy, targeted therapy) does not recreate the original healthy tissue. The tumour microenvironment is fundamentally remodeled, immune cell populations are re-organised, stromal architecture is altered, and surviving normal cells have undergone stress-induced epigenetic changes [46]. What is achieved is a new stable state a re-organised regulatory equilibrium corresponding to D_7 (signature (0, 1, 2), three flows still intact). The persistence of this state (durable remission) depends on whether the post-treatment cusp structure is truly stable or whether perturbations can push the system back toward PV_{deg} (minimal residual disease recurrence). Exceptionally deep remissions, in which the tissue approaches its pre-malignant functional identity, may correspond to the further $D_7 \rightarrow D_8$ transition.

7.2.3. Neuroplasticity and recovery from brain injury

Following stroke, traumatic brain injury, or neurodegenerative progression, functional recovery occurs through neuroplasticity, the re-organisation of neural circuits to compensate for lost function [47]. The recovered state is not a restoration of the original neural architecture but a new stable configuration of re-organised connectivity. A Nash equilibrium of the post-injury neural network. Therapeutic strategies that enhance neuroplasticity (constraint-induced movement therapy, neurostimulation, cognitive rehabilitation) can be understood as interventions that facilitate the $PV_{deg} \rightarrow D_7$ transition by providing the perturbation energy needed to escape the autistic trap.

7.2.4. Distinction between Nash recovery and return to D_6

Table 3 distinguishes the two recovery modes:

Table 3: Comparison between full D_6 health restoration and Nash recovery (PIII(D_7), signature (0, 1, 2)). Unlike the erroneous picture of D_7 as having fewer flows, both D_6 and D_7 preserve all three independent dynamical channels; they differ in cusp count and balance.

Feature	D_6 restoration	Nash recovery (D_7)
Target state	Original health state	New reorganised equilibrium
Signature	(0, 2, 2)	(0, 1, 2)
Degrees of freedom	3 holes	3 holes (preserved)
Cusps	4 (symmetric)	3 (partially rebalanced)
Route	Therapy reverting pathological change	PVdeg → D7 (enrichment of binding)
Continuation	Can deepen via D6 → D7 → D8	Can deepen further via D7 → D8
Clinical examples	Acute infection resolved; Cancer remission; wound scar; rapid reperfusion after ischaemia	Cancer remission; wound scar; post-stroke plasticity; psychiatric recovery
Reversibility	Full	Partial

8. Consciousness, Cognition, and the PV Health Interface

8.1. Painlevé V in consciousness model's

A striking and non-trivial consequence of the present framework is its connection to mathematical models of consciousness. In [13], it was shown that consciousness dynamics can be modeled by a four-manifold Painlevé V system, in which gamma oscillations (∼40 Hz) arise as the physical signature of the PV critical state.

The three degeneration channels from PV correspond to distinct cognitive and affective states**.** This is not an incidental parallel. In the integrated information theory of consciousness [48] and in free-energy minimization models [49], the "healthy" cognitive state is precisely one of balanced**,** self-correcting prediction error minimization a D_6 type attractor. Psychopathologies can be interpreted as autistic traps (PV_{deg} depression, addiction, OCD states of metastable confinement within a suboptimal but stable cognitive attractor) or regulatory collapses (PIV, psychosis, mania, severe epilepsy).

8.2. The health consciousness continuum

The relationship between health and consciousness is bidirectional and well-established clinically (psychoneuroimmunology, psychosomatic medicine). In the Painlevé framework this bidirectionality has a natural explanation, both biological regulation (at the molecular and physiological levels) and cognitive regulation (at the neural and psychological levels) are governed by the same hierarchy of confluence transitions, operating at different scales but sharing the same topological structure.

Specifically:

1. ***Psychoneuroimmunological coupling***: Chronic psychological stress (a PV_{deg} cognitive state) drives HPA axis dysregulation and systemic low-grade inflammation (a PV_{deg} physiological state) through shared neuroendocrine and cytokine pathways [50].

2. ***Mind-body recovery***: Interventions targeting cognitive regulation (mindfulness, CBT, physical exercise) can shift the cognitive system from PV_{deg} toward D_6 or D_7, with measurable downstream effects on immune function and metabolic parameters a cascade of Nash transitions across scales.

3. ***Biofeedback and neurostimulation***: Technologies such as transcranial magnetic stimulation (TMS), deep brain stimulation (DBS), and neurofeedback can be understood as direct cusp-signature modifiers at the neural circuit level, with therapeutic effects arising from topological transitions in neural regulatory space.

8.3. AI and extended health monitoring

In [14], the Painlevé confluence framework was applied to human-AI collaboration dynamics, with 1/f phase-locking as the physical correlate of the PV critical state in joint cognitive systems. This extension suggests that AI systems modeling biological regulatory networks may themselves operate near PV-type critical states, and that the mathematical framework described here may apply to the dynamical monitoring of health through AI-mediated time-series analysis of biological signals. Specifically, the proximity of a patient's regulatory network to the PV_{deg} versus D_6 regime might be detectable from statistical properties of physiological time series (e.g., heart rate variability, EEG spectral structure, miRNA expression variance) that reflect the underlying cusp signature.

9. Perspectives for Quantum Biology and Medicine

9.1. Cusp signatures as topological biomarkers

The central operational proposal of this article is that cusp signatures may serve as topological biomarkers of biological health status. Unlike conventional molecular biomarkers (concentrations of specific proteins, gene expression levels), cusp signatures are invariants of the global dynamical architecture they describe the topology of the regulatory landscape, not its molecular content.

This proposal has several testable implications:

1. Two samples with identical molecular profiles (transcriptomics, proteomics) but different network topologies (as assessed by connectivity, feedback loop structure, and monodromy analysis) should exhibit different long-term dynamics and disease trajectories.

2. Therapeutic interventions that modify the cusp signature

(e.g., by altering network connectivity through miRNA mimics/inhibitors, epigenetic drugs, or signaling network rewiring) should have qualitatively different effects from those that merely shift molecular concentrations without changing network topology.

3. Dynamical signatures of approach to the PV critical point the 1/f spectral signature identified geometrically via WKB/Stokes analysis of Painlevé V confluence and arithmetically via the Mangoldt function in phase-locked loop dynamics [14] should be detectable in biological time series as early warning signals of impending $D_6 \to PV_{deg}$ or $PV_{deg} \to PIV$ transitions. The disappearance of this 1/f signature in physiological time series (e.g., heart rate variability, EEG, cytokine fluctuation rhythms) may signal onset of the autistic trap. By contrast, recovery toward D_7 should be marked by the reappearance of broad-band 1/f fluctuations as the system re-engages creative regulatory dynamics.

9.2. Mathematical program

A rigorous mathematical programme is needed to extract cusp signatures from biological data. Preliminary directions include:

1. Network monodromy analysis is developing computational methods to extract the SL(2,C) monodromy representation of a given regulatory network from single-cell RNA-seq or spatial transcriptomics data, and to identify the associated character variety and cusp signature.

2. ***Isomonodromy deformation tracking***: Using time-resolved multi-omic data to track how the character variety parameters deform during disease progression, identifying PVI→PV→{D_6, PV_{deg}, PIV} transitions in real biological time.

3. ***Topological data analysis***: Applying persistent homology and Morse theory to high dimensional biological state spaces to detect the characteristic topological features (bifurcation points, unstable manifolds) associated with Painlevé transitions.

9.3. Experimental tests

The most direct experimental tests would focus on biological systems with known bistable dynamics:

1. ***EMT model systems***: MCF10A cells undergoing TGF-β-induced EMT provide a well characterised example of a PVI→PV transition. Single-cell RNA-seq time courses during this transition could be analysed for characteristic PV dynamics in the miR-200/ZEB mutual inhibition network.

2. ***Dormancy models***: Established in vitro and in vivo cancer dormancy models (e.g., prostate cancer micrometastasis in bone marrow) could be characterised at the level of miRNA network topology to test whether dormant cells occupy a PV_{deg} type state.

3. ***Metabolic switching***: The transition from aerobic to anaerobic metabolism during exercise or hypoxia, and back, involves well-characterised regulatory switching that may exhibit PV type critical dynamics in the HIF-1α and AMPK regulatory networks.

10. Conclusion

We have proposed a mathematical framework for biological health and disease grounded in the Painlevé confluence hierarchy and the cusp-signature classification of decorated character varieties.

The key elements are:

1. The PVI→PV confluence models the emergence of biological criticality: the transition from a multi-flow progenitor state to a bipolar decision node analogous to a quantum bit. The cusp signature changes from (0, 0, 0, 0) to (0, 0, 2), encoding the appearance of competing binding interactions.

2. From PV, three channels lead to qualitatively distinct health outcomes: quantum health (PIII(D_6), signature (0, 2, 2)), the autistic trap (PV_{deg}, signature (0, 0, 1)), and regulatory collapse (PIV, signature (0, 4)). The D-type integrative pathway $D_6 \to D_7 \to D_8$ deepens health regulation progressively, preserving all three flows while balancing cusp distribution toward the minimal symmetric signature (0, 1, 1) of D_8.

3. The shared character variety of D_6 and PV_{deg} provides a precise geometric explanation for phenomena such as cancer dormancy, chronic inflammation, and epigenetic locking: the autistic trap is not a different landscape but a different cusp configuration within the same landscape.

4. Nash recovery ($PV_{deg} \to D_7$, signature (0, 1, 2), three flows preserved) describes biological repair as the escape from metastable confinement into a re-organised equilibrium with enriched and partially rebalanced cusp structure. The term honours John Nash's life trajectory of recovery from paranoid schizophrenia an archetype of escaping a metastable cognitive autistic trap rather than any game-theoretic concept.

5. The same mathematical structure governs consciousness dynamics at the neural level and regulatory dynamics at the molecular and physiological levels, suggesting a deep mathematical unity across scales.

The framework is explicitly predictive, it calls for topological biomarkers based on cusp signatures extractable from biological data, early-warning signals of Painlevé transitions, and

therapeutic strategies that modify network topology rather than merely shifting molecular concentrations. The connection to established physical results (PV in Bose-Einstein correlations, random matrix level spacing, and gamma oscillations) provides non-trivial physical grounding for a proposal that might otherwise appear purely metaphorical.

We hope that this work will stimulate a dialogue between Painlevé geometry, quantum biology, systems medicine, and mathematical psychiatry fields that the quantum health framework suggests are united by a common topological language.

References

1. Kitano H. Biological robustness. Nat Rev Genet. 2004;5:826-837.
2. Scheffer M, et al. Early-warning signals for critical transitions. Nature. 2009;461:53-59.
3. Ferrell JE. Bistability, bifurcations, and Waddington's epigenetic landscape. Curr Biol. 2012;22:R458-R466.
4. Huang S, Eichler G, Bar-Yam Y, Ingber DE. Cell fates as high-dimensional attractor states of a complex gene regulatory network. Phys Rev Lett. 2005;94:128701.
5. Li C, Wang J. Quantifying cell fate decisions for differentiation and reprogramming of a human stem cell network: landscape and biological paths. PLoS Comput Biol. 2013;9:e1003165.
6. Lambert N, et al. Quantum biology. Nat Phys. 2013;9:10-18.
7. Romero E, et al. Quantum coherence in photosynthesis for efficient solar-energy conversion. Nat Phys. 2014;10:676-682.
8. Forrester PJ. Log-gases and random matrices. Princeton: Princeton University Press; 2010.
9. Chekhov L, Mazzocco M, Rubtsov V. Painlevé monodromy manifolds, decorated character varieties and cluster algebras. Int Math Res Not. 2017;2017:7639-7691.
10. Planat M. Topology and dynamics of transcriptome (dys)regulation. Int J Mol Sci. 2024;25:4971.
11. Planat M. The qubit as a Painlevé V critical state: Fricke character varieties and topological collapse channels. Quantum Inf Comput. 2026; (in press).
12. Planat M. Topological symmetry breaking in consciousness dynamics: from human geniuses to AI systems. Symmetry. 2026;18:427.
13. Planat M. Consciousness as 4-manifold Painlevé V dynamics: from quantum topology to classical gamma oscillations. Axioms. 2026;15:124.
14. Planat M. Painlevé confluence and 1/f phase-locking dynamics: a topological framework for human–AI collaboration. Mach Learn Knowl Extr. 2026;8:73.
15. Bost JB, Connes A. Hecke algebras, type III factors and phase transitions with spontaneous symmetry breaking in number theory. Selecta Math. 1995;1:411-457.
16. Bonelli G, Lisovyy O, Maruyoshi K, Sciarappa A, Tanzini A. On Painlevé/gauge theory correspondence. Lett Math Phys. 2017;107:2359-2412.
17. Jimbo M, Miwa T. Monodromy preserving deformation of linear ordinary differential equations with rational coefficients II. Physica D. 1981;2:407-448.
18. Clarkson PA. Painlevé transcendents. In: DLMF Handbook of Mathematical Functions. Cambridge: Cambridge University Press; 2010.
19. Okamoto K. Studies on the Painlevé equations. Ann Mat Pura Appl. 1987;146:337-381.
20. van der Put M, Saito M. Moduli spaces for linear differential equations and the Painlevé equations. Ann Inst Fourier. 2009;59:2611-2667.
21. Jimbo M, Miwa T, Mori Y, Sato M. Density matrix of an impenetrable Bose gas and the fifth Painlevé transcendent. Physica D. 1980;1:80-158.
22. Dyson FJ. Statistical theory of the energy levels of complex systems I. J Math Phys. 1962;3:140-156.
23. Tracy CA, Widom H. Fredholm determinants, differential equations and matrix models. Commun Math Phys. 1994;163:33-72.
24. Boalch P. From Klein to Painlevé via Fourier, Laplace and Jimbo. Proc Lond Math Soc. 2005;90:167-208.
25. Cantat S, Loray F. Dynamics on character varieties and Malgrange irreducibility of Painlevé VI. Ann Inst Fourier. 2009;59:2927-2978.
26. Bartel DP. MicroRNAs: target recognition and regulatory functions. Cell. 2009;136:215-233.
27. Lahav G, et al. Dynamics of the p53-Mdm2 feedback loop in individual cells. Nat Genet. 2004;36:147-150.
28. Hat B, Kochańczyk M, Bogdał MN, Lipniacki T. Feedbacks, bifurcations, and cell fate decision-making in the p53 system. PLoS Comput Biol. 2016;12:e1004787.
29. Lev Bar-Or R, et al. Generation of oscillations by the p53-Mdm2 feedback loop: a theoretical and experimental study. Proc Natl Acad Sci USA. 2000;97:11250-11255.
30. Nieto MA, et al. EMT: 2016. Cell. 2016;166:21-45.
31. Bracken CP, Gregory PA, Kolesnikoff N, Bert AG, Wang J, Shannon MF, Goodall GJ. A double-negative feedback loop between ZEB1-SIP1 and the microRNA-200 family regulates epithelial–mesenchymal transition. Cancer Res. 2008;68:7846-7854.
32. Wherry EJ. T cell exhaustion. Nat Immunol. 2011;12:492-499.
33. Volinia S, et al. A microRNA expression signature of human solid tumors defines cancer gene targets. Proc Natl Acad Sci USA. 2006;103:2257-2261.
34. Tili E, et al. Modulation of miR-155 and miR-125b levels following lipopolysaccharide/TNF-α stimulation and their possible roles in regulating the response to endotoxin shock. J Immunol. 2007;179:5082-5089.
35. Poy MN, et al. miR-375 maintains normal pancreatic α- and β-cell mass. Proc Natl Acad Sci USA. 2009;106:5813-5818.
36. Downward J. Targeting RAS signalling pathways in cancer therapy. Nat Rev Cancer. 2003;3:11-22.
37. Mehta P, et al. COVID-19: consider cytokine storm syndromes and immunosuppression. Lancet. 2020;395:1033-1034.
38. DeLorenzo RJ, et al. Epidemiology of status epilepticus. J Clin Neurophysiol. 1995;12:316-325.
39. Wang J, Zhang K, Xu L, Wang E. Quantifying the Waddington landscape and biological paths for development and differentiation. Proc Natl Acad Sci USA. 2011;108:8257-8262.
40. Campbell JE, Drucker DJ. Pharmacology, physiology, and mechanisms of incretin hormone action. Cell Metab. 2013;17:819-837.
41. Takahashi K, Yamanaka S. Induction of pluripotent stem cells from mouse embryonic and adult fibroblast cultures by defined factors. Cell. 2006;126:663-676.
42. Aguirre-Ghiso A. Models, mechanisms and clinical evidence for cancer dormancy. Nat Rev Cancer. 2007;7:834-846.
43. Hotamisligil GS. Inflammation and metabolic disorders. Nature. 2006;444:860-867.
44. Baylin SB, Jones PA. A decade of exploring the cancer epigenome biological and translational implications. Nat Rev Cancer. 2011;11:726-734.
45. Gurtner GC, et al. Wound repair and regeneration. Nature. 2008;453:314-321.
46. Zou W. Immunosuppressive networks in the tumour environment and their therapeutic relevance. Nat Rev Cancer. 2005;5:263-274.
47. Cramer SC, et al. Harnessing neuroplasticity for clinical applications. Brain. 2011;134:1591-1609.
48. Tononi G. An information integration theory of consciousness. BMC Neurosci. 2004;5:42.
49. Friston K. The free-energy principle: a unified brain theory? Nat Rev Neurosci. 2010;11:127-138.
50. Dantzer R, et al. From inflammation to sickness and depression: when the immune system subjugates the brain. Nat Rev Neurosci. 2008;9:46-56.